Eur. J. Mineral.
2017, **29**, 315–322
Published online 14 October 2016

Zincostrunzite, $ZnFe^{3+}_2(PO_4)_2(OH)_2{\cdot}6.5H_2O$, a new mineral from the Sitio do Castelo mine, Portugal, and the Hagendorf-Süd pegmatite, Germany

ANTHONY R. KAMPF[1,*], IAN E. GREY[2], PEDRO ALVES[3], STUART J. MILLS[4], BARBARA P. NASH[5], COLIN M. MACRAE[2] and ERICH KECK[6]

[1] Mineral Sciences Department, Natural History Museum of Los Angeles County, 900 Exposition Boulevard, Los Angeles, CA 90007, USA
*Corresponding author, e-mail: akampf@nhm.org
[2] CSIRO Mineral Resources, Private Bag10, Clayton South 3169, VIC, Australia
[3] Landscape, Heritage and Territory Laboratory (Lab2PT), University of Minho, Braga, Portugal
[4] Geosciences, Museum Victoria, GPO Box 666, Melbourne 3001, VIC, Australia
[5] Department of Geology and Geophysics, University of Utah, Salt Lake City, UT 84112, USA
[6] Algunderweg 3, 92694 Etzenricht, Germany

Abstract: Zincostrunzite (IMA2016-023), $ZnFe^{3+}_2(PO_4)_2(OH)_2{\cdot}6.5H_2O$, is a new secondary phosphate mineral from the Sitio do Castelo tungsten mine in Portugal and the Hagendorf-Süd pegmatite in Germany. At Sitio do Castelo, zincostrunzite was derived from the alteration of triplite–zwieselite. At Hagendorf-Süd, it was found in a nodule of former triphylite that had been replaced by phosphophyllite and minor apatite. At Sitio do Castelo, zincostrunzite occurs as prisms up to 2 mm long. At Hagendorf-Süd, the mineral makes up portions of needles that are up to about 5 mm long. Crystals are elongated on [0 0 1] with the prism forms {0 1 0} and {1 $\overline{1}$ 0} and poorly formed terminations, probably {0 0 1}. Twinning is ubiquitous by 180° rotation on [0 1 0] with the composition plane {1 $\overline{2}$ 0}. Zincostrunzite crystals from Sitio do Castelo are light brownish yellow; those from Hagendorf-Süd are silvery white. The lustre is vitreous to silky and the streak is white. Crystals are brittle with irregular, splintery fracture and at least one perfect cleavage parallel to [0 0 1]; probably either {1 $\overline{1}$ 0} or {1 0 0}. The Mohs' hardness is about 2½. The measured density (Sitio do Castelo) is 2.66(1) g cm^{-3}. At room temperature, the mineral is slowly soluble in dilute HCl and rapidly soluble in concentrated HCl. Optically, crystals are biaxial (−), with $\alpha = 1.620(2)$, $\beta = 1.672(2)$, $\gamma = 1.720(2)$ (white light); $2V_{meas.} = 89.5(5)°$; $2V_{calc.} = 85.1°$; orientation is $Z \wedge \mathbf{c} = 3°$; $X \approx \mathbf{a}^*$; pleochroism is X nearly colourless, Y light brownish yellow, Z darker brownish yellow ($X < Y < Z$). Electron-microprobe analyses gave the empirical formulas $(Zn_{0.74}Mn^{2+}_{0.23})_{\Sigma 0.97}Fe^{3+}_{1.99}(PO_4)_2(OH)_2{\cdot}6.5H_2O$ (Sitio do Castelo) and $(Zn_{0.93}Mn^{2+}_{0.08})_{\Sigma 1.01}(Fe^{3+}_{1.84}Mn^{2+}_{0.19})_{\Sigma 2.03}(PO_4)_2(OH)_2{\cdot}6.5H_2O$ (Hagendorf-Süd). Zincostrunzite is triclinic, $P\overline{1}$, with $a = 10.1736(6)$, $b = 9.7999(5)$, $c = 7.3296(2)$ Å, $\alpha = 91.325(4)°$, $\beta = 97.895(6)°$, $\gamma = 116.948(4)°$, $V = 642.22(6)$ Å^3 and $Z = 2$. The eight strongest lines in the X-ray powder diffraction pattern are [d_{obs}/Å (I) (h k l)]: 8.87 (100) (100, 010, 1 $\overline{1}$ 0), 5.32 (95) (1 $\overline{1}$ 1, 011), 4.457 (30) (200), 4.287 (41) (020, $\overline{2}$ 2 0), 3.310 (29) (120, $\overline{2}$ $\overline{1}$ 1), 3.220 (75) (multiple), 1.9116 (25) (multiple) and 1.6222 (32) (multiple). The crystal structure was refined to $R_1 = 0.0715$ for 3243 observed reflections [$F_o > 4\sigma F$] for a crystal from Sitio do Castelo. The mineral is isostructural with other members of the strunzite group, except for an additional split H_2O site near the (½,0,0) centre of symmetry, which accounts for the additional 0.5 H_2O in the ideal formula. The extra H_2O site may be present in some crystals of other strunzite-group minerals, as its presence cannot be determined without a structure refinement.

Key-words: zincostrunzite; new mineral; crystal structure; phosphate; Sitio do Castelo mine; Portugal; Hagendorf-Süd pegmatite; Germany.

1. Introduction

Strunzite was first described sixty years ago from the Hagendorf-Süd pegmatite in Germany (Frondel, 1957). It has since been found at numerous localities worldwide, as have the two other members of the strunzite group, ferrostrunzite (Peacor *et al.*, 1983) and ferristrunzite (Peacor *et al.*, 1987). Herein, we describe the fourth member of the group, zincostrunzite, which was collected by one of the authors (EK) at Hagendorf-Süd in 1977 and was recently discovered by another of the authors (PA) at the Sitio do Castelo mine in Portugal. Comparative data for all four members of the strunzite group are provided in Table 1.

The name zincostrunzite reflects the fact that this is the Zn analogue of strunzite, $Mn^{2+}Fe^{3+}_2(PO_4)_2(OH)_2{\cdot}6H_2O$, with Zn replacing Mn^{2+}. The mineral and name (IMA2016-023) were approved by the IMA–CNMNC prior to publication. The description is based upon three cotype specimens. Two cotypes from the Sitio do Castelo mine are housed in the collections of the Mineral Sciences Department, Natural History Museum of Los Angeles

DOI: 10.1127/ejm/2017/0029-2593
0935-1221/17/0029-2593 $ 3.60

Table 1. Comparative data for strunzite-group minerals.

	Strunzite	Ferrostrunzite	Ferristrunzite	Zincostrunzite
Ideal formula	$Mn^{2+}Fe^{3+}{}_2(PO_4)_2(OH)_2{\cdot}6H_2O$	$Fe^{2+}Fe^{3+}{}_2(PO_4)_2(OH)_2{\cdot}6H_2O$	$Fe^{3+}Fe^{3+}{}_2(PO_4)_2(OH)_3{\cdot}5H_2O$	$ZnFe^{3+}{}_2(PO_4)_2(OH)_2{\cdot}6.5H_2O$
Crystal system	Triclinic	Triclinic	Triclinic	Triclinic
Space group	$P\overline{1}$	$P\overline{1}$	$P\overline{1}$	$P\overline{1}$
a (Å)	10.228(5)	10.17–10.23	10.01(2)	10.1736(6)
b (Å)	9.837(5)	9.77–9.78	9.73(2)	9.7999(5)
c (Å)	7.284(5)	7.37–7.40	7.334(8)	7.3296(2)
α (°)	90.17(5)	88.63–89.65	90.50(12)	91.325(4)
β (°)	98.44(5)	97.60–98.28	96.99(10)	97.895(6)
γ (°)	117.44(5)	117.26–117.60	116.43(10)	116.948(4)
Z	2	2	2	2
Strongest lines in X-ray powder pattern in Å	9.02(10) 5.32(8) 4.50(5) 4.35(6) 4.27(6) 3.29(6) 3.23(6)	8.94(80) 5.29(100) 4.47(30) 4.33(20) 3.452(30) 3.277(40) 3.213(30)	8.87(80) 5.34(100) 4.48(20) 4.20(30) 3.442(30) 3.387(30) 3.267(40)	8.87(100) 5.32(95) 4.457(30) 4.287(41) 3.310(29) 3.220(75) 1.9116(25) 1.6222(32)
D_{meas} (g cm^{-3})	2.52(5)	2.50	2.38–2.50	2.66(1)
D_{calc} (g cm^{-3})	2.49	2.57	2.55	2.655
Opt. character	Biaxial (–)	Biaxial (–)	Biaxial (–)	Biaxial (–)
α	1.619–1.625	1.628(2)	1.664(4)	1.620(2)
β	1.640–1.670	1.682(calc)	1.698(calc)	1.672(2)
γ	1.696–1.720	1.723(4)	1.757(5)	1.720(2)
$2V_{meas}$ (°)	56–93	80(5)	77(10)	89.5(5)
Reference	Anthony *et al.* (2015)	Anthony *et al.* (2015)	Anthony *et al.* (2015)	This work

County, 900 Exposition Boulevard, Los Angeles, CA 90007, USA, catalogue numbers 65646 and 65647. One cotype from Hagendorf-Süd is housed in the Geosciences collections at Museum Victoria, Melbourne, Australia, registration number M53585.

2. Occurrence

Zincostrunzite occurs at two localities, the Sitio do Castelo mine, Folgosinho, Gouveia, Guarda District, Portugal (40°30′41″ N, 7°30′29″ W) and the Hagendorf-Süd pegmatite, Hagendorf, Oberpfalz, Bavaria, Germany (49°39′1″ N, 12°27′35″ E). These deposits are considered cotype localities for the species.

The Sitio do Castelo mine exploits a wolframite-bearing quartz lens. It was worked for tungsten from 1917 through the end of World War II (officially declared abandoned in 1972). It was reopened in 1976 and exploited for quartz until 1986 (officially declared abandoned in 1998). The deposit is well-known to collectors for its diverse suites of unusual secondary phosphate minerals, which have formed as the result of intense weathering of primary triplite–zwieselite, fluorapatite and isokite in association with sulfide minerals, *e.g.* sphalerite, arsenopyrite and chalcopyrite (Alves *et al.*, 2012). Two types of secondary phosphate assemblages occur in the deposit. The first type is derived from the alteration of triplite–zwieselite yielding, in order of abundance, phosphosiderite, strengite, rockbridgeite–frondelite, cacoxenite, bermanite, beraunite, strunzite, stewartite, laueite, leucophosphite, benyacarite, fluorapatite, wavellite and kidwellite. The second type is derived from the alteration of triplite–zwieselite in association with fluorapatite and isokite yielding, in order of abundance, ludlamite, vivianite, strunzite, Zn-rich rockbridgeite–frondelite, Mn-rich phosphophyllite, hydroxylapatite, jahnsite-(CaMnFe), earlshannonite, lunokite and plimerite. The new mineral zincostrunzite occurs in vugs in the second type of secondary phosphate assemblage on matrix composed of triplite–zwieselite, fluorapatite and cryptomelane. Other minerals found in direct association with zincostrunzite are cacoxenite, plimerite, strengite and strunzite. Zincostrunzite has been found as crystals that are completely zincostrunzite as well as crystals that are mostly strunzite, but with zincostrunzite rims.

At the Hagendorf-Süd pegmatite, the new mineral occurs on the 67 metre level of the Cornelia mine open cut, where it was collected from a 30 × 40 × 50 cm nodule of former triphylite that had been replaced by vivianite, phosphophyllite and minor apatite. Zincostrunzite is only

found in portions of crystals that otherwise fall in the composition range of strunzite (or ferristrunzite). These crystals occur as one of the youngest phases in a cavity mostly containing more-or-less-altered phosphophyllite crystals. Other secondary minerals found in the cavity include chalcophanite, Sr-bearing fluorapatite, hopeite (as epitactic overgrowths on phosphophyllite), jahnsite, Zn-bearing laueite, mitridatite, parahopeite, pseudo-laueite, scholzite–parascholzite, schoonerite, stewartite and whitmoreite–earlshannonite. Goethite and cryptomelane are also abundant in the oxidized zone. The secondary phosphate paragenesis at the pegmatite is described in detail by Mücke (1981), but obviously does not include the minerals described after 1981.

3. Physical and optical properties

At Sitio do Castelo, zincostrunzite occurs as prisms up to 2 mm long, typically intergrown in sub-parallel bundles (Fig. 1). At Hagendorf-Süd, the mineral makes up portions of needles that are up to about 5 mm long. These needles form bundles and divergent sprays (Fig. 2). The crystals are elongated on [0 0 1] with poorly formed terminations. The forms observed are {0 1 0}, {1 $\bar{1}$ 0} and probably {0 0 1} (Fig. 3). Twinning is ubiquitous by 180° rotation on [0 1 0] with the composition plane {1 $\bar{2}$ 0}.

Zincostrunzite crystals from Sitio do Castelo are light brownish yellow; those from Hagendorf-Süd are silvery white. Crystals are transparent with a vitreous to silky lustre and white streak. The mineral is non-fluorescent. Crystals are brittle with irregular, splintery fracture, and at least one perfect cleavage parallel to [0 0 1]; probably either {1 $\bar{1}$ 0} or {1 0 0}. The Mohs' hardness is about 2½, based upon scratch tests. The density of crystals from Sitio do Castelo measured by floatation in aqueous sodium polytungstate solution is 2.66(1) g cm^{-3}. The calculated density is 2.655 g cm^{-3} using the empirical formula and single-crystal unit cell (Sitio do Castelo) and 2.679 g cm^{-3} for the ideal formula. At room temperature, the mineral is slowly soluble in dilute HCl (minutes) and rapidly soluble in concentrated HCl (seconds).

Optically, zincostrunzite crystals are biaxial (−), with $\alpha = 1.620(2)$, $\beta = 1.672(2)$, $\gamma = 1.720(2)$, measured in white light. The measured $2V$ is 89.5(5)° from extinction data using EXCALIBR (Gunter *et al.*, 2004); the calculated $2V$ is 85.1°. Dispersion could not be observed. The partially determined optical orientation is $Z \wedge \mathbf{c} = 3°$; $X \approx \mathbf{a}^*$. Crystals are pleochroic: X = nearly colourless, Y = light brownish yellow, Z = darker brownish yellow; $X < Y < Z$. The Gladstone–Dale compatibility (Mandarino, 2007) is 0.039, in the range of excellent compatibility, based upon the empirical formula (Sitio do Castelo).

4. Chemical composition

Chemical analyses of zincostrunzite from Sitio do Castelo (9 points on 1 crystal) were carried out using a Cameca SX-50 electron microprobe in the Department of Geology and Geophysics at the University of Utah (wavelength-dispersive mode, 15 kV, 10 nA, 10 μm beam diameter) utilizing Probe for EPMA software. Raw X-ray intensities were corrected for matrix effects with a $\phi(\rho z)$ algorithm (Pouchou & Pichoir, 1991). Chemical analyses of zincostrunzite portions of crystals from Hagendorf-Süd (4 points) were carried out using a JEOL JXA 8500F Hyperprobe at CSIRO Mineral Resources, Victoria, Australia (WDS mode, 12 kV, 4 nA, 2 μm beam diameter). Raw X-ray intensities were corrected for matrix effects with a $\phi(\rho z)$ algorithm implemented in the JEOL system. All Fe is reported as trivalent (Fe_2O_3), as indicated by the results of the structure refinement and bond-valence analysis. The very large standard deviations for MnO and Fe_2O_3 for the Hagendorf-Süd analyses reflect substitution of Mn for Fe. This suggests that Mn might be trivalent in

Fig. 1. Bundles of zincostrunzite prisms with strengite (purple) and cacoxenite (yellow balls) on plimerite (black) from Sitio do Castelo; field of view 1.7 mm across. (Online version in colour.)

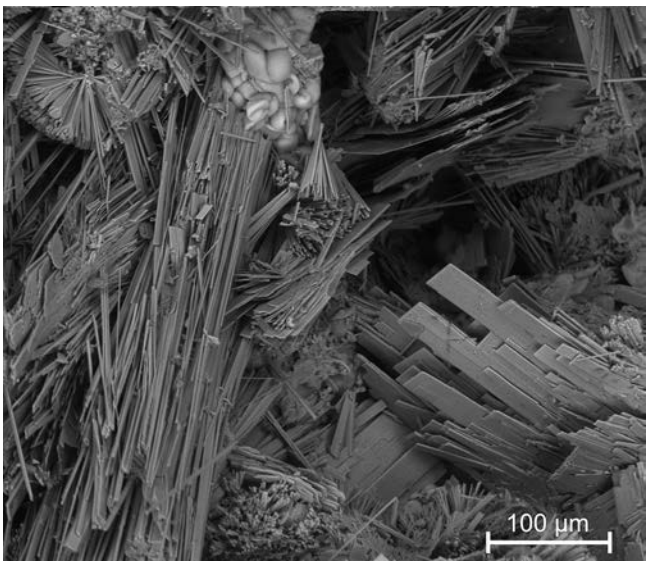

Fig. 2. Back-scatter SEM image of zincostrunzite needles (left) with schoonerite blades (right) from Hagendorf-Süd.

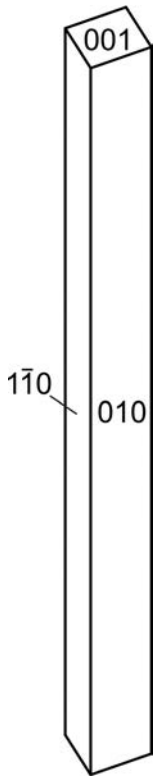

Fig. 3. Crystal drawing of zincostrunzite from Sitio do Castelo (clinographic projection).

the Hagendorf-Süd zincostrunzite; however, this is counter-indicated by the presence of associated minerals containing both di- and trivalent Fe, *e.g.* schoonerite, which is consistent with less oxidizing conditions than are required for Mn^{3+}.

There was insufficient material for CHN analyses, so H_2O was calculated on the basis of P = 2, charge balance and 16.5 O *apfu*, as determined by the crystal structure analysis (see below). The analyses totals are high, probably as the result of the loss under vacuum of some loosely held H_2O. Analytical data are given in Table 2.

Based on 16.5 O *apfu*, the empirical formula for material from Sitio do Castelo is $(Zn_{0.74}Mn^{2+}_{0.23})_{\Sigma 0.97}Fe^{3+}_{1.99}(PO_4)_2(OH)_2{\cdot}6.5H_2O$ (+0.09 H) and the for material from Hagendorf-Süd is $(Zn_{0.93}Mn^{2+}_{0.08})_{\Sigma 1.01}(Fe^{3+}_{1.84}Mn^{2+}_{0.19})_{\Sigma 2.03}(PO_4)_2(OH)_2{\cdot}6.5H_2O$ (+0.08 H). The ideal formula is $ZnFe^{3+}_2(PO_4)_2(OH)_2{\cdot}6.5H_2O$, which requires ZnO 15.71, Fe_2O_3 30.82, P_2O_5 27.40, H_2O 26.08, total 100 wt.%.

5. X-ray crystallography and crystal-structure determination

Powder X-ray diffraction data for zincostrunzite from Sitio do Castelo were obtained on a Rigaku R-Axis Rapid II curved–imaging-plate microdiffractometer utilising monochromatised Mo$K\alpha$ radiation. A Gandolfi-like motion on the φ and ω axes was used to randomize the sample. Observed *d* values and intensities were derived by profile fitting using JADE 2010 software (Materials Data Inc.). Data are given in Table 3. The unit-cell parameters refined from the powder data using JADE 2010 with whole-pattern fitting are: $a = 10.190(10)$, $b = 9.778(10)$, $c = 7.338(11)$ Å, $\alpha = 91.21(2)°$, $\beta = 97.96(2)°$, $\gamma = 116.99(4)°$ and $V = 642.3(2)$ Å^3.

Table 2. Analytical data (in wt.%) for zincostrunzite.

Constituent	Mean	Range	SD	Probe standard
Sitio do Castelo				
ZnO	12.07	10.38–13.63	1.25	Synthetic ZnO
MnO	3.28	1.02–4.70	1.30	Rhodonite
Fe_2O_3	32.00	31.20–32.63	0.46	Hematite
P_2O_5	28.53	27.77–29.05	0.38	Apatite
H_2O*	27.30			
Total	103.18			
Hagendorf-Süd				
ZnO	15.13	14.46–15.83	0.58	Phosphophyllite
MnO	3.74	0.00–7.36	4.16	Rhodonite
Fe_2O_3	29.23	22.97–32.97	4.50	Hematite
P_2O_5	28.24	27.57–29.27	0.77	Berlinite
H_2O*	27.02			
Total	103.39			

* Based on the structure.

Single-crystal structure data were obtained on the same instrument noted above using a crystal from Sitio do Castelo. Crystals of zincostrunzite from Sitio do Castelo (as well as zoned crystals of strunzite–zincostrunzite from Hagendorf-Süd) are ubiquitously twinned and of poor diffraction quality. The TwinSolve program within the Rigaku CrystalClear software package was used for processing of HKLF 5 structure data, including the application of an empirical multi-scan absorption correction using ABSCOR (Higashi, 2001). Note that the averaging of reflections by TwinSolve combined equivalent reflections with positive and negative *h* indices; consequently, only reflections with positive *h* indices are reported. The atom positions for Al-bearing strunzite (Grey *et al.*, 2012) were used as the starting point for the structure refinement, which employed SHELXL-2013 software (Sheldrick, 2015).

The Zn site was refined with joint occupancy by Zn and Mn resulting in $Zn_{0.79}Mn_{0.21}$, in good agreement with the empirical formula. An additional H_2O site, OW7, was found, split by 0.92(4) Å across the centre of symmetry at (½,0,0). This site refined to close to half occupancy and was assigned 0.5 occupancy in the final refinement, yielding one additional H_2O group per unit cell (½ H_2O *pfu*). Efforts to locate the 16 H atom sites yielded possible positions for only 6, some of which provided ambiguous and/or dubious hydrogen bonds. Ultimately, we concluded that the problems inherent in integrating reflections of a twinned lattice for a crystal of poor diffraction quality precluded the reliable determination of any H atom positions. In the final stages of refinement, we still encountered large residuals and numerous disagreeable reflections, the 15 worst of which were omitted from the

Table 3. Powder X-ray diffraction data (*d* in Å) for zincostrunzite from Sitio do Castelo.

I_{obs}	d_{obs}	d_{calc}	I_{calc}	*hkl*
100	8.87	8.9433	69	1 0 0
		8.6949	14	0 1 0
		8.4889	17	-1 1 0
		5.8420	2	0-1 1
95	5.32	5.3388	55	1-1 1
		5.3107	45	0 1 1
		5.1583	4	1 1 0
6	4.95	5.0295	5	-2 1 0
		4.8967	3	-1 2 0
30	4.457	4.4716	21	2 0 0
41	4.287	4.3474	24	0 2 0
		4.2444	22	-2 2 0
11	4.068	4.0881	6	1-2 1
6	3.931	4.0200	6	-1 2 1
		3.9240	2	1 1 1
		3.8962	3	2-1 1
11	3.559	3.5756	7	0 2 1
		3.5630	5	2-2 1
21	3.422	3.4570	10	0-1 2
		3.4027	14	-1 1 2
29	3.310	3.3498	15	1 2 0
		3.2835	17	-2-1 1
75	3.220	3.2562	14	-3 2 0
		3.2514	8	1-1 2
		3.2277	19	-1 3 0
		3.2105	15	-3 1 1
		3.1982	2	-1-1 2
		3.1954	10	-2 3 0
		3.1722	11	1 0 2
14	3.074	3.0703	19	-2 0 2
13	2.762	2.7670	16	1 1 2
10	2.681	2.7031	5	-2-1 2
		2.6523	10	-3 1 2
12	2.600	2.6069	7	2 0 2
		2.5791	10	2 2 0
10	2.511	2.5147	6	-4 2 0
		2.4847	3	-3-1 1
		2.4776	2	-4 2 1
12	2.454	2.4664	3	1-3 2
		2.4554	2	-4 1 0
		2.4463	4	1 3 0
20	2.370	2.4079	5	-2 3 2
		2.3795	9	2-3 2
		2.3779	2	-4 3 0
		2.3757	5	0-3 2
		2.3519	2	-1 3 2
		2.3445	3	-3 4 0
23	2.307	2.3317	9	2-4 1
		2.3062	3	-2 4 1
		2.3045	2	1 2 2
		2.2992	4	-3 3 2
		2.2922	3	-2 1 3
8	2.234	2.2420	2	3 1 1
		2.2358	4	4 0 0
		2.2224	3	4-1 1
		2.1990	3	0-2 3
8	2.168	2.1737	2	0 4 0
		2.1394	3	0-4 1
		2.1222	3	-4 4 0
		2.0961	2	-1-2 3
12	2.0605	2.0647	2	1 1 3
		2.0603	2	-4 0 2
		2.0561	2	3 2 0
		2.0458	3	-3 2 3
		2.0282	2	0 4 1
		1.9744	2	-5 3 1
		1.9586	2	4 1 0
		1.9530	2	-2 5 0
25	1.9116	1.9190	3	1 4 0
		1.9158	7	1 3 2
		1.9074	2	3 1 2
		1.9032	7	4-3 2
		1.8987	2	4-1 2
		1.8974	2	-2-3 2
11	1.8665	1.8746	3	3-5 1
		1.8685	2	-2 5 1
		1.8662	4	-5 4 0
15	1.8303	1.8320	3	-5 1 2
		1.8307	7	-1 0 4
		1.8278	5	2 1 3
7	1.7871	1.7901	2	-1 1 4
		1.7867	3	-1-4 2
		1.7741	2	4 0 2
14	1.7148	1.7225	2	-5 4 2
		1.7164	3	1 0 4
		1.7149	2	1-5 2
		1.7049	3	1-2 4
		1.6968	3	-3 1 4
11	1.6709	1.6850	3	-1 2 4
		1.6765	4	-5 5 1
		1.6754	2	3 2 2
		1.6729	2	-3 0 4
		1.6585	2	3-4 3
		1.6418	5	-4-2 2
32	1.6222	1.6322	6	-3 6 0
		1.6297	4	0-5 2
		1.6257	3	2-2 4
		1.6210	4	4-5 2
		1.6200	3	-1 5 2
		1.6139	3	0 2 4
		1.6115	2	5 1 0
		1.6052	2	-6 2 2
		1.6043	2	0-3 4
7	1.5802	1.5968	4	-6 1 0
		1.5763	2	1 5 0
		1.5753	3	-5 5 2
		1.5448	2	4-4 3
9	1.5057	1.5115	3	3-2 4
		1.5067	4	5 0 2
		1.5006	2	5-5 2
		1.4905	3	6 0 0
		1.4797	2	-3-2 4
11	1.4644	1.4679	2	3 3 2
		1.4664	2	2-4 4
		1.4625	2	1-6 2
		1.4608	2	-2-3 4
		1.4546	2	-4-1 4
15	1.4468	1.4501	2	6-3 2
		1.4485	2	0-1 5
		1.4458	2	-4-3 2
		1.4426	2	3 0 4
		1.4413	2	-2 4 4
		1.4395	5	-5 1 4
5	1.4200	1.4208	4	-5 6 2

Note: Calculated lines with intensities less than 2 are not shown.

final refinement. Details of data collection and structure refinement are provided in Table 4. Fractional coordinates and atom displacement parameters are provided in Table 5, selected interatomic distances in Table 6 and bond valences in Table 7. The Crystallography Information File (CIF), including reflection data, is available online as supplementary material linked to this article on the GSW website of the journal, http://eurjmin.geoscienceworld.org.

Table 4. Data collection and structure refinement details for zincostrunzite from Sitio do Castelo.*

Diffractometer	Rigaku R-Axis Rapid II
X-ray radiation/power	Mo$K\alpha$ ($\lambda = 0.71075$ Å)/50 kV, 40 mA
Temperature	293(2) K
Structural formula	$(Zn_{0.79}Mn^{2+}_{0.21})_{\Sigma 1.00}Fe^{3+}_2$ $(PO_4)_2(OH)_2{\cdot}6.5H_2O$
Space group	$P\bar{1}$
Unit-cell dimensions	$a = 10.1736(6)$ Å
	$b = 9.7999(5)$ Å
	$c = 7.3296(2)$ Å
	$\alpha = 91.325(4)°$
	$\beta = 97.895(6)°$
	$\gamma = 116.948(4)°$
V	642.22(6) Å^3
Z	2
Density (for above formula)	2.668 g cm^{-3}
Absorption coefficient	4.238 mm^{-1}
F(000)	515.94
Crystal size	$270 \times 55 \times 30$ μm
θ range	2.28–25.03°
Index ranges	$0 \le h \le 12$, $-11 \le k \le 10$, $-8 \le l \le 8$
Reflections collected/unique	3914/3914
Reflections with $F_o > 4\sigma F$	3243
Completeness to θ = 25.03°	96.2 %
Max. and min. transmission	0.394 and 0.883
Refinement method	Full-matrix least-squares on F^2
Parameters refined	202
GoF	1.070
Final R indices [$F_o > 4\sigma F$]	$R_1 = 0.0715$, w$R_2 = 0.2259$
R indices (all data)	$R_1 = 0.0840$, w$R_2 = 0.2356$
Extinction coefficient	0.005(5)
Largest diff. peak/hole	+1.35/−1.18 e/Å^3

* $R_{int} = \Sigma|F_o^2 - F_o^2(\text{mean})|/\Sigma[F_o^2]$. GoF = $S = \{\Sigma[w(F_o^2 - F_c^2)^2]/(n-p)\}^{1/2}$. $R_1 = \Sigma||F_o| - |F_c||/\Sigma|F_o|$. $wR_2 = \{\Sigma[w(F_o^2 - F_c^2)^2]/\Sigma[w(F_o^2)^2]\}^{1/2}$. $w = 1/[\sigma^2(F_o^2) + (aP)^2 + bP]$ where a is 0.1611, b is 4.4164 and P is $[2F_c^2 + \text{Max}(F_o^2, 0)]/3$.

6. Discussion of the structure

The structure (Fig. 4) contains one $ZnO_2(H_2O)_4$ octahedron, two distinct $Fe^{3+}O_3(OH)_2(H_2O)$ octahedra, two distinct PO_4 tetrahedra and an unconnected H_2O group. The Fe-centred octahedra are *trans*-corner-linked through OH forming chains along [0 0 1]. The chains are linked to one another *via* corner-sharing with PO_4 tetrahedra to form sheets parallel to {1 0 0}. The sheets are linked in the [1 0 0] direction by corner-sharing with

Table 6. Selected bond distances (Å) in zincostrunzite from Sitio do Castelo.

Zn–O7	2.018(8)	Fe1–OH2	1.958(8)	Fe2–O8	1.879(7)
Zn–O1	2.023(8)	Fe1–OH1	1.962(7)	Fe2–OH2	2.021(8)
Zn–OW4	2.138(10)	Fe1–O2	1.962(8)	Fe2–OH1	2.029(8)
Zn–OW1	2.157(9)	Fe1–O5	1.975(7)	Fe2–OW5	2.060(8)
Zn–OW2	2.157(8)	Fe1–O4	2.030(8)	Fe2–O3	2.065(8)
Zn–OW3	2.177(8)	Fe1–OW6	2.204(9)	Fe2–O6	2.067(8)
<Zn–O>	2.112	<Fe1–O>	2.015	< Fe2–O>	2.020
P1–O2	1.502(8)	Hydrogen bonds			
P1–O1	1.527(8)	OH1–O3	2.864(11)	OW4–O6	3.017(13)
P1–O3	1.553(8)	OH2–O5	2.827(11)	OW4–OW7	2.68(3)
P1–O4	1.580(8)	OW1–O4	2.915(12)	OW5–OW2	2.816(12)
<P1–O>	1.541	OW1–OW3	2.858(12)	OW5–OW4	3.191(13)
		OW2–O3	2.789(11)	OW6–O6	2.705(11)
P2–O8	1.499(7)	OW2–O7	2.921(12)	OW6–OW7	2.79(3)
P2–O5	1.538(8)	OW3–O1	2.832(12)	OW7–O1	2.88(2)
P2–O6	1.550(8)	OW3–O7	2.662(12)	OW7–OW6	2.78(3)
P2–O7	1.569(9)				
<P2–O>	1.539				

Table 5. Atom fractional coordinates and displacement parameters (Å^2) for zincostrunzite from Sitio do Castelo.

Site	x	y	z	U_{eq}	U^{11}	U^{22}	U^{33}	U^{23}	U^{13}	U^{12}
Zn*	0.49478(15)	0.32866(16)	0.25776(19)	0.0137(6)	0.0135(9)	0.0161(9)	0.0128(8)	0.0016(6)	0.0047(5)	0.0073(6)
Fe1	0.97548(17)	0.24538(18)	0.13642(19)	0.0097(5)	0.0135(9)	0.0124(9)	0.0061(8)	0.0008(6)	0.0013(6)	0.0085(7)
Fe2	0.03156(16)	0.77429(18)	0.36396(19)	0.0089(5)	0.0125(9)	0.0103(9)	0.0059(8)	0.0004(6)	0.0016(6)	0.0070(7)
P1	0.8050(3)	0.4580(3)	0.0682(4)	0.0086(7)	0.0092(14)	0.0094(14)	0.0095(13)	0.0008(11)	0.0007(10)	0.0064(11)
P2	0.1870(3)	0.1558(3)	0.4381(4)	0.0084(7)	0.0104(14)	0.0089(14)	0.0071(13)	−0.0003(10)	0.0012(10)	0.0058(11)
O1	0.6377(9)	0.3736(10)	0.0747(11)	0.0193(18)	0.012(4)	0.029(5)	0.017(4)	−0.003(4)	0.004(3)	0.010(4)
O2	0.8491(9)	0.3350(9)	0.0262(10)	0.0141(17)	0.024(4)	0.016(4)	0.009(4)	0.001(3)	0.005(3)	0.015(4)
O3	0.8972(9)	0.5486(9)	0.2567(10)	0.0129(16)	0.018(4)	0.015(4)	0.006(4)	0.000(3)	0.001(3)	0.008(3)
O4	0.8365(9)	0.5697(9)	0.9095(11)	0.0143(17)	0.018(4)	0.012(4)	0.015(4)	0.002(3)	0.003(3)	0.009(3)
O5	0.0866(9)	0.1405(9)	0.2536(10)	0.0133(16)	0.018(4)	0.019(4)	0.010(4)	0.005(3)	0.001(3)	0.015(3)
O6	0.1816(9)	−0.0025(9)	0.4680(10)	0.0142(17)	0.021(4)	0.016(4)	0.009(4)	0.000(3)	−0.001(3)	0.012(4)
O7	0.3490(9)	0.2872(10)	0.4355(11)	0.0198(19)	0.017(4)	0.021(5)	0.012(4)	−0.007(3)	0.001(3)	0.001(4)
O8	0.1359(9)	0.2003(9)	0.6016(10)	0.0127(16)	0.018(4)	0.020(4)	0.006(3)	−0.002(3)	0.003(3)	0.014(3)
OH1	0.9668(9)	0.3119(9)	0.3871(10)	0.0136(17)	0.021(4)	0.019(4)	0.007(4)	−0.002(3)	0.003(3)	0.015(4)
OH2	0.0427(9)	0.8500(10)	0.1097(10)	0.0154(17)	0.021(4)	0.019(4)	0.009(4)	0.003(3)	0.005(3)	0.012(4)
OW1	0.3172(10)	0.2499(11)	0.0225(12)	0.023(2)	0.023(5)	0.033(5)	0.015(4)	0.004(4)	0.004(3)	0.015(4)
OW2	0.6795(9)	0.4350(10)	0.4838(11)	0.0180(18)	0.018(4)	0.019(4)	0.017(4)	0.003(3)	0.000(3)	0.009(4)
OW3	0.5140(11)	0.5578(10)	0.2345(12)	0.0237(19)	0.036(5)	0.018(5)	0.021(4)	−0.001(4)	−0.002(4)	0.018(4)
OW4	0.4686(12)	0.1053(12)	0.3131(15)	0.036(2)	0.040(6)	0.026(5)	0.045(6)	0.011(5)	0.012(5)	0.016(5)
OW5	0.2227(9)	0.7595(10)	0.3313(11)	0.0188(18)	0.021(4)	0.025(5)	0.016(4)	−0.003(3)	0.000(3)	0.017(4)
OW6	0.2266(9)	−0.0338(10)	−0.1663(11)	0.0198(18)	0.020(4)	0.022(5)	0.016(4)	0.000(3)	0.003(3)	0.008(4)
OW7*	0.523(3)	0.048(2)	−0.019(4)	0.041(6)	0.037(14)	0.036(15)	0.046(14)	−0.010(13)	0.005(10)	0.015(13)

* Occupancies: Zn/Mn = 0.79/0.21(4); OW7 = 0.5.

Table 7. Bond-valence analysis for zincostrunzite from Sitio do Castelo. Values are expressed in valence units.

	Zn	Fe1	Fe2	P1	P2	Hydrogen bonds	Σ
O1	0.45			1.28		+0.17, +0.16	2.06
O2		0.58		1.36			1.94
O3			0.44	1.19		+0.16, +0.19	1.98
O4		0.48		1.11		+0.15	1.74
O5		0.56			1.24	+0.17	1.97
O6			0.43		1.20	+0.13, +0.22	1.98
O7	0.45				1.14	+0.15, +0.25	1.99
O8			0.72		1.38		2.10
OH1		0.58	0.48			–0.18	0.88
OH2		0.58	0.49			–0.20	0.87
OW1	0.31					–0.15, –0.16	0.00
OW2	0.31					+0.18, –0.19, –0.15	0.15
OW3	0.29					+0.16, –0.17, –0.25	0.03
OW4	0.33					+0.10, –0.13, –0.24	0.06
OW5			0.44			–0.10, –0.18	0.16
OW6		0.30				+0.19, –0.22, –0.19	0.08
OW7						+0.24, +0.19, –0.16, –0.19	0.08
Σ	2.14	3.08	3.00	4.94	4.96		

* The bond strengths for the Zn site are based upon its refined occupancy, $Zn_{0.79}Mn^{2+}{}_{0.21}$. Fe^{3+}–O, Zn^{2+}–O and Mn^{2+}–O bond-valence parameters are from Brown & Altermatt (1985) and P^{5+}–O are from Brese & O'Keeffe (1991). Hydrogen-bond strengths based on O–O bond distances from Ferraris & Ivaldi (1988).

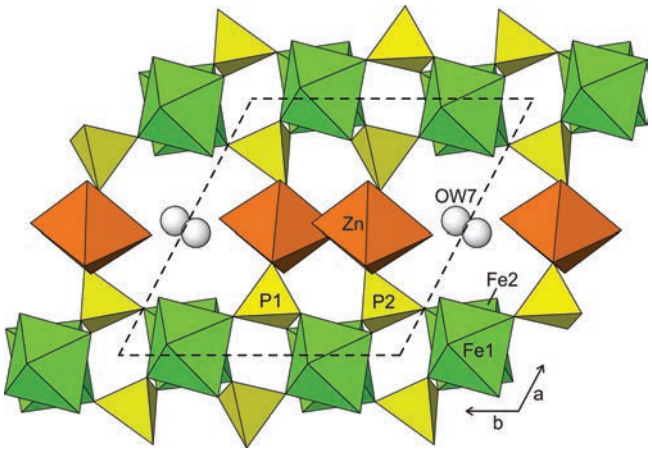

Fig. 4. The structure of zincostrunzite viewed along [0 0 1]. (Online version in colour.)

the Zn-centred octahedra forming a framework with cavities centred at the (½,0,0) centre of symmetry. The unconnected H_2O group occupies a split site in the cavity. An extensive system of hydrogen bonds further links the structural components.

The hydrogen bonds reported by Grey *et al.* (2012) for Al-bearing strunzite were based upon determined H positions and, as such, have stronger foundation than those we propose for zincostrunzite; however, the hydrogen bonding scheme in Al-bearing strunzite is not entirely compatible with the zincostrunzite structure because of geometrical differences between the structures and the addition of the unconnected OW7 site in zincostrunzite. The hydrogen bonds in zincostrunzite that differ from those in Al-bearing strunzite (given in parentheses) are OW1–O4 (OW1–O5), OW2–O7 (OW2–OW3), OW3–O1 (OW3–OW2), OW4–O6 (none), OW4–OW7 (none), OW5–OW4 (OW5–OW2) and OW6–OW7 (OW6–OW1). Note that Grey *et al.* (2012) do not list hydrogen bonds from OW4 because they found none with donor–acceptor distances less than 3 Å.

We also collected data for a Zn-bearing ferristrunzite from Hagendorf-Süd on the macromolecular beam line MX2 of the Australian Synchrotron. The structure refinement for this dataset also indicated an additional split H_2O site. We plan a complete description of this structure refinement for a future publication, in which we will compare it in detail with the zincostrunzite structure and those of other strunzite-group structures that do not have the additional H_2O site.

An additional isolated H_2O site found in the structures of both zincostrunzite from Sitio do Castelo and Zn-bearing ferristrunzite from Hagendorf-Süd arguably could qualify these phases as distinct from their counterparts without an additional H_2O site. Unfortunately, without a structure determination or a very accurate direct water determination, it is impossible to conclusively determine whether a crystal of a strunzite-group mineral contains an extra H_2O site. Furthermore, because structure refinements have never been done on type-specimen crystals of strunzite, ferrostrunzite and ferristrunzite, it is not known whether they contain an additional H_2O site. Consequently, for practical reasons, we suggest that the presence of the isolated H_2O site in the strunzite structure type not be considered to be species determining. The general formula for M^{2+} (Mn^{2+}, Fe^{2+}, Zn) members of the strunzite group can be given as $M^{2+}Fe^{3+}{}_2(PO_4)_2(OH)_2{\cdot}6–6.5H_2O$ or $M^{2+}Fe^{3+}{}_2(PO_4)_2(OH)_2(H_2O)_6{\cdot}0–0.5H_2O$, while that for M^{3+} (currently only Fe^{3+}) members of the strunzite group can be given as $M^{3+}Fe^{3+}{}_2(PO_4)_2(OH)_3{\cdot}5–5.5H_2O$ or

$M^{3+}Fe^{3+}{}_2(PO_4)_2(OH)_3(H_2O)_5{\cdot}0–0.5H_2O$. These formulas are based on $Z = 2$ for consistency and comparison with previously used formulas for strunzite-group minerals. As noted above, the additional H_2O site is a two-fold, half-occupied site, which accounts for one H_2O group per unit cell.

Acknowledgements: The paper benefited from comments by Andrey Zolotarev and an anonymous reviewer. This study was funded, in part, by the John Jago Trelawney Endowment to the Mineral Sciences Department of the Natural History Museum of Los Angeles County.

References

Alves, P., Leal Gomes, C., Lopes Nunes, J.E. (2012): Produtos de evolução de triplite-zwieselite, fluorapatite e isokite da mina Sítio do Castelo (Folgosinho, Guarda). II Congresso Jovens Investigadores em Geociências, LEG 2012.

Anthony, J.W., Bideaux, R.A., Bladh, K.W., Nichols, M.C., eds. (2015): "Handbook of Mineralogy". Mineralogical Society of America, Chantilly, VA 20151-1110, USA. http://www.handbookofmineralogy.org/.

Brese, N.E. & O'Keeffe, M. (1991): Bond-valence parameters for solids. *Acta Cryst., B*, **47**, 192–197.

Brown, I.D. & Altermatt, D. (1985): Bond-valence parameters from a systematic analysis of the inorganic crystal structure database. *Acta Cryst., B*, **41**, 244–247.

Ferraris, G. & Ivaldi, G. (1988): Bond valence vs. bond length in OO hydrogen bonds. *Acta Cryst., B*,**44**, 341–344.

Frondel, C. (1957): Strunzit, ein neues Mineral. *Naturwiss*, **45**, 37–38.

Grey, I.E., Macrae, C.M., Keck, E., Birch, W.D. (2012): Aluminium-bearing strunzite derived from jahnsite at the Hagendorf-Süd pegmatite, Germany. *Mineral. Mag.*, **76**, 1165–1174.

Gunter, M.E., Bandli, B.R., Bloss, F.D., Evans, S.H., Su, S.C., Weaver, R. (2004): Results from a McCrone spindle stage short course, a new version of EXCALIBR, and how to build a spindle stage. *Microscope*, **52**, 23–39.

Higashi, T. (2001): ABSCOR. Rigaku Corporation, Tokyo.

Mandarino, J.A. (2007): The Gladstone-Dale compatibility of minerals and its use in selecting mineral species for further study. *Can. Mineral.*, **45**, 1307–1324.

Mücke, A. (1981): The paragenesis of the phosphate minerals of the Hagendorf pegmatite – a general view. *Chemie der Erde*, **40**, 217–234.

Peacor, D.R., Dunn, P.J., Simmons, W.B. (1983): Ferrostrunzite, the ferrous iron analogue of strunzite from Mullica Hill, New Jersey. *Neues Jahrb. Mineral., Monatsh.*, **1983**, 524–528.

Peacor, D.R., Dunn, P.J., Simmons, W.B., Ramik, R.A. (1987): Ferristrunzite, a new member of the strunzite group, from Blaton, Belgium. *Neues Jahrb. Mineral., Monatsh.*, **1987**, 433–440.

Pouchou, J.-L. & Pichoir, F. (1991): Quantitative analysis of homogeneous or stratified microvolumes applying the model "PAP". *in* "Electron probe quantitation", K.F.J. Heinrich and D.E. Newbury, eds. Plenum Press, New York, 3l–75.

Sheldrick, G.M. (2015): Crystal structure refinement with SHELXL. *Acta Cryst., C*, **71**, 3–8.

Received 23 June 2016
Modified version received 2 September 2016
Accepted 5 September 2016